Journal of Assisted Reproduction and Genetics (2024) 41:109–120
https://doi.org/10.1007/s10815-023-02966-x

GENETICS

A novel *NPHP4* homozygous missense variant identified in infertile brothers with multiple morphological abnormalities of the sperm flagella

Asim Ali[1,2] · Ahsanullah Unar[1] · Zubair Muhammad[1] · Sobia Dil[1] · Beibei Zhang[1] · Humaira Sadaf[3] · Manan Khan[4] · Muhammad Ali[2] · Ranjha Khan[1] · Kakakhel Mian Basit Shah[2] · Ao Ma[1] · Xiaohua Jiang[1] · Yuanwei Zhang[1] · Huan Zhang[1] · Qinghua Shi[1]

Received: 29 May 2023 / Accepted: 3 October 2023 / Published online: 13 October 2023

Abstract

Purpose Asthenozoospermia is an important cause of male infertility, and the most serious type is characterized by multiple morphological abnormalities of the sperm flagella (MMAF). However, the precise etiology of MMAF remains unknown. In the current study, we recruited a consanguineous Pakistani family with two infertile brothers suffering from primary infertility due to MMAF without obvious signs of PCD.

Methods We performed whole-exome sequencing on DNAs of the patients, their parents, and a fertile brother and identified the homozygous missense variant (c.1490C > G (p.P497R) in *NPHP4* as the candidate mutation for male infertility in this family.

Results Sanger sequencing confirmed that this mutation recessively co-segregated with the MMAF in this family. In silico analysis revealed that the mutation site is conserved across different species, and the identified mutation also causes abnormalities in the structure and hydrophobic interactions of the NPHP4 protein. Different bioinformatics tools predict that *NPHP4*$^{p.P497R}$ mutation is pathogenic. Furthermore, Papanicolaou staining and scanning electron microscopy of sperm revealed that affected individuals displayed typical MMAF phenotype with a high percentage of coiled, bent, short, absent, and/or irregular flagella. Transmission electron microscopy images of the patient's spermatozoa revealed significant anomalies in the sperm flagella with the absence of a central pair of microtubules (9 + 0) in every section scored.

Conclusions Taken together, these results show that the homozygous missense mutation in *NPHP4* is associated with MMAF.

Keywords WES · MMAF · Male infertility · *NPHP4* · Central pair

Introduction

Male infertility is one of the leading health concerns in the world. In fact, approximately 15% of couples at the age of reproductive capacity are unable to conceive after 1 year of unprotected sexual contact [1]. More than half of all infertility cases are caused by male factors, characterized primarily by quantitative defects in the sperm [2, 3]. On the other hand, there are still approximately 20–40% of male infertility cases that are considered to be idiopathic [4]. These unexplained cases are thought to be caused by rare genetic mutations affecting the intricate process of spermatogenesis, and mutations in more than 1000 genes associated with germ cell enriched expression might lead to defective spermatogenesis [5].

Accordingly, asthenozoospermia is a major cause of infertility and is defined as a reduction in motility of ejaculated spermatozoa, which occurs due to defects in the

✉ Asim Ali
asim21pk@ustc.edu.cn

✉ Qinghua Shi
qshi@ustc.edu.cn

[1] Division of Reproduction and Genetics, The First Affiliated Hospital of University of Science and Technology of China, School of Basic Medical Sciences, Division of Life Sciences and Medicine, Biomedical Sciences and Health Laboratory of Anhui Province, University of Science and Technology of China, Hefei 230027, China

[2] Department of Biotechnology, COMSATS University Islamabad, Abbottabad Campus, Abbottabad 22060, Pakistan

[3] Department of Obstetrics and Gynecology, Ayub Medical Hospital Complex, Abbottabad, Pakistan

[4] Department of Biotechnology and Genetic Engineering, Hazara University, Mansehra, Pakistan

ultrastructure of sperm flagella, such as missing of central pair (CP) of microtubules or a defect in the arrangement of nine peripheral microtubule doublets surrounding CP (9 + 2) [6]. The CPs have an important role during spermiogenesis in maintaining the overall structure of flagellum, specially the absence of CPs leads to an abnormal "9 + 0" configuration of the axoneme, and is found to be the major defect occurring in most MMAF cases [7]. The presence of such defects has also been observed in affected individuals with mutations in genes such as *DNAH1*, *FSIP2*, *AK7*, *ARMC2*, *STK33*, *DNAH8*, *and QRICH2* [8–14], which were further supported with experimental models that indicated structural defects affecting CPs contribute to the development of MMAF [15]. However, these genetic findings account for approximately 60% of the MMAF cases [16], and more genetic factors need to be studied to understand the pathogenesis of MMAF thoroughly.

A highly conserved protein, nephrocystin-4 encoded by NPHP4, plays a critical role in ciliary function and structure. An autosomal recessive kidney disorder characterized by mutations in *NPHP4* is associated with vision or brain defects [17]. Recently, Alazami et al. reported the presence of *NPHP4* homozygous variants that were associated with severe male infertility in familial case. This is the first report of male infertility associated with *NPHP4* [18]. Although *NPHP4* mutations are associated with male infertility in different ethnicities, however, the underlying genetic causes are still not fully understood.

The current study involved a consanguineous Pakistani family with two infertile individuals having asthenozoospermia. Based on WES analysis, a homozygous missense mutation was identified in the *NPHP4* gene (p.P497R). The Sanger sequencing of *NPHP4* variants confirmed that *NPHP4* p.P497R was associated with infertility phenotype in patients. Further investigations using *in silico* and electron microscopy analyses of patient spermatozoa confirmed the MMAF phenotype caused by the absence of CPs in patient spermatozoa. Till now, it is the first study reporting the importance of *NPHP4* that regulate the ultrastructure of human spermatozoa associated with the formation of CP and added a new *NPHP4* missense variant to the gene-mutation pool associated with male infertility and MMAF.

Material and methods

Clinical information of participants

In present study, we enrolled two male infertile patients from a consanguineous Pakistani family. Before beginning this study, all family members provided written informed consent. The participants completed a detail questionnaire regarding their infertility history and physical information. To rule out associated disorders, including renal manifestations, renal function test and routine urine examination have been performed. Both affected individuals have no signs or symptoms of PCD according to clinical observations. In accordance with WHO guidelines, semen analyses were performed from each patient, including semen volume, sperm concentration, sperm motility, and sperm morphology [19]. The blood samples of all members of the family collected were used to carried out hormonal analysis and karyotyping. This study was approved by the ethical committee of the University of Science and Technology of China.

Papanicolaou staining of sperm smears slides

Spermatozoa were smeared on a clean slide and fixed with 4% paraformaldehyde followed by three washes with 1 × PBS. The Papanicolaou staining of the semen smear slides was performed as per the WHO protocol, with a few modifications noted below [19]. Smear slides were initially dehydrated in different concentrations of alcohol gradient (90–30% ethanol) and ddH2O for 1 min. Next, dipped in solution A (Harris' hematoxylin) and solution B (acidic ethanol) for 4 to 8 min each, followed by washing with water after each step. Smear slides were rehydrated in 50–95% ethanol, dipped in solution C (Orange G6), 95% ethanol three times, and in solution D (EA-50 green dye), 95–100% ethanol twice before being dehydrated in xylene. A natural balsam sealant was used to seal the slides, and a cover slip was placed over them. Images were taken using a laser scanning confocal microscope (Olympus).

Transmission electron microscopy (TEM) and scanning electron microscopy (SEM)

To analyze the ultrastructure organization of the patient's spermatozoa, SEM and TEM analyses were carried out as described previously [20]. In brief, spermatozoa were fixed overnight at 4 °C in 0.1 M phosphate buffer (PB; pH 7.4) containing 4% paraformaldehyde, 8% glutaraldehyde, and 0.2% picric acid. After a further wash with 0.1 M buffer for four times, the fixed spermatozoa samples were post-fixed with 1% OsO4 and dehydrated, followed by infiltration of acetone and epon resin mixture. After embedding the samples, ultrathin sections of approximately 70 nm were cut by an ultrathin microtome before staining with uranyl acetate and lead citrate. Tecnai 10 and 12 Microscopes [21] at 100 kV or 120 kV, or the Hitachi H-7650 microscope at 100 kV were used to examine the ultrastructure of the samples.

Whole-exome sequencing and data analysis

According to the manufacturer, AI Exome Enrichment Kit V1 (iGeneTech, Beijing, China) derived libraries were created for exome capture of all available family members (III:1 III:2 IV:1, IV:2, IV:3, IV:4). The sequencing was conducted using the Illumina Hiseq2000 platform (San Diego, CA, USA). Filtration of the variants was performed as described below. (1) Variants potentially affecting protein sequence were retained. (2) Variants with minor allele frequencies (MAF) > 0.01 in any of the public databases, 1000 Genome project (http://www.internationalgenome.org/) [22], ESP6500 (http://evs.gs.washington.edu/) [23].

Specifically, variants homozygous in our imputation of variant calls from 578 fertile men (41 Pakistanis, 254 Chinese, and 283 Europeans) extracted from ExAC (http://exac.broadinstitute.org) [24] or GnomAD (http://gnomad.broadinstitute.org) [25], and (2) variants potentially predicted as non-deleterious by more than half of imputation algorithms [26, 27–34] covering them were excluded. (4) Variants within genes that are not expressed in the testes were excluded. (5) Variants that follow inheritance patterns were included. (6) Variants within genes that may be important in spermatogenesis based on FertilityOnline or literature were included (Figure S1) [35]. A Sanger sequencing analysis of genomic DNA from all available family members was performed in order to validate the mutant genes identified by WES. In Supplementary Table S1, primers used for Sanger sequencing analysis are listed.

In silico analysis

In this study, we aimed to investigate the function and pathogenicity of the missense mutation p.P497R in *NPHP4*. The *NPHP4* genomic sequences were retrieved from the NCBI database (http//ncbi.nlm.nih.gov). To predict the pathogenicity of the identified mutation, we used various online pathogenicity prediction bioinformatics tools including PolyPhen-1, PolyPhen-2, PROVEAN, SIFT, Align GV-GD, FATHMM, PhD-SNP, MAPP, Mutation Assessor, SNAP-2 and Mutation Taster [28, 30, 36–54]. To assess the stability of the NPHP4 protein, we used two bioinformatics tools, namely I-Mutant and Mutant Pro [55–58]

The NPHP4 protein structure was obtained from the Alphafold protein structure database, a deep-Mind artificial intelligence system that predicts the three-dimensional structure of proteins based on their amino acid sequences. To analyze the effect of the mutation on protein structure, we used FoldX, and HOPE was employed for automatic mutant analysis. The structures were visualized and analyzed using PyMol [59]. Furthermore, multiple sequence alignments of the NPHP4 protein and the evolutionary conservation of the mutated residue across different species were performed using MEGA7 [60, 61].

Statistical analysis

Student's *t*-test was performed for investigation of different defects in spermatozoa between control and patients. The results were presented as mean ± SEM.

Results

Clinical investigations of affected individuals

The infertility treatment was offered to a consanguineous Pakistani family with two male patients suffering from primary infertility at a local hospital in Abbottabad, Pakistan. Both patients (P1:IV:3 and P2:IV:4) have normal height and secondary sexual characteristics but failed to produce offspring even after trying to conceive during > 6 years of marriage (Table 1). These patients have normal visceral positions without signs or symptoms of PCD (Figure S2) (Table S4). Neither patient had a history of testicular damage, infection, or radiotherapy or chemotherapy. All reproductive hormones tested in the patients (Table 1) were within normal ranges. An examination of the chromosomes revealed a normal karyotype, and no Y-chromosome microdeletions were detected in either patient's somatic cells. Hormonal analyses for both patients showed normal ranges (P1:IV:3 FSH (10.11 mIU/mL), LH:9.92 mIU/mL), prolactin 14.48 (ng/mL), testosterone (8.48 ng/mL), and P2:IV:4 FSH (7.30 mIU/mL), (LH:4.21 mIU/mL), (prolactin 8.1 ng/m) (Table1). Both patients (P1:IV:3 and P2:IV:4) as well as one fertile brother (IV:5) had semen examination performed according to WHO recommendations. As a result of the semen analyses, patients IV: 3 (9.50 ± 12.30) and IV: 4 (20 ± 7.07) showed reduced motility as compared to control and were therefore diagnosed as asthenozoospermia (Table 1). The sperm morphology was determined by Pap staining on sperm smears slides, and more than 200 spermatozoa were captured, and images were taken using a digital Nikon DS-Ri1 camera mounted on a Nikon Eclipse 80i microscope. The sperm morphology analysis indicated that 90% of the spermatozoa displayed defective sperm flagella, including missing, absent, and coiled (Table 1) (Fig. 1B, C), which confirmed the asthenozoospermia phenotype with MMAF.

Identification of a novel homozygous missense *NPHP4* variant in patients with asthenoteratozoospermia

In the clinical investigations of both affected patients, asthenozoospermia with MMAF was diagnosed. The aim of this study was to identify the genetic causes of

Table 1 Clinical investigations of patients carrying the *NPHP4* mutation

Parameters	Reference values	Patient IV:3	Patient IV:4	Control IV:5
Age (years)	-	46	31	20
Height (cm)/weight (kg)	-	165.1/70	170.2/66	170.1/65
BMI	18.5–24.9	25.68	22.78	22.44
Age (y) of marriage	-	22	14	06
Chest X-ray		Normal	Normal	Normal
Ultrasonography				
Left testis size (cm)	3.6–5.5 × 2.1–3.5	3.51 × 2.91	3.84 × 2.88	-
Right testis size (cm)	3.6–5.5 × 2.1–3.5	3.29 × 2.35	3.69 × 2.23	-
Renal function test				
Urea (mg/dL)		42	31	-
Creatinine (mg/dL)	Upto 1.2	1	1.1	-
Uric acid (mg/dL)		5	5.2	-
Urine protein		Trace	(+)	-
Hormone analysis				
FSH (mIU/mL)	1.0–11	7.3	10.11	-
LH (mIU/mL)	1.0–8.0	4.21	9.92	-
Prolactin (ng/mL)	3.00–14.70	8.17	15.48	-
Testosterone (ng/mL)	3–10	5.18	8.48	-
Semen analysis				
Ejaculate volume (mL)	> 1.5	2.5 ± 0.83	3.16 ± 0.81	3.5
pH	7.2–7.8	7.65 ± 0.17	7.96 ± 0.08	7.5
Sperm concentration (10^6/mL)	> 15	29.16 ± 7.3	15.16 ± 7.62	28
Motility				
Total motility PR + NP (%)	> 40	20 ± 7.07	9.50 ± 12.30	33
Progressive motility PR (%)	> 32	6.5 ± 2.73	2.5 ± 4.1	18
Vitality (%)	> 58	35 ± 14.14	40	42
Morphology				
Normal spermatozoa (%)	> 4	7.42 ± 3.13	5.95	64.9
Normal head (%)	> 23	61.99 ± 3.00	48.68	67.06
Normal flagella (%)	> 23	14.36 ± 1.70	18.81	39.71
Aberrant flagella (%)	-	85.63 ± 1.70	81.18	60.2
Absent flagella (%)	-	2.08 ± 0.47	6.93	1.82
Short flagella (%)	-	30.28 ± 5.14	10.23	11.34
Coiled flagella (%)	-	28.24 ± 4.71	37.62	28.36
Bent flagella (%)	-	19.75 ± 4.36	22.12	19.38
Irregular flagella (%)	-	5.26 ± 3.31	4.29	0.7

Reference values for hormones analysis and Renal Function Tests were established by the local laboratory based on the normal individuals of patient's population. Reference limits (5th centiles and their 95% confidence intervals) according to the World Health Organization standard 2010, and the distribution range of morphologically normal spermatozoa observed in fertile individuals

PR progressive motility, *NP* non-progressive motility

asthenozoospermia in infertile patients by assessing all the available family members, including both patients (IV:3 and IV:4), their parents (III:1 and III:2), and one control brother (IV:5). Following a series of criteria, genetic variants were filtered. A flow chart diagram in Supplementary Figure 1 presents a complete strategy for analyzing WES data for a family. In brief, as the individuals were born to a consanguineous family, variants following recessive inheritance pattern in the sequenced family members were considered of priority. The variants meeting the following conditions were given preference: (1) variants potentially affecting protein sequence; (2) variants with minor allele frequency (MAF) < 0.01 in the 1000 Genomes, ESP6500, ExAC, and Genome Aggregation Database; (3) loss-of-function variants or potentially deleterious missense variants predicted by software including Sorting Intolerant From Tolerant, PolyPhen-2, and Mutation Taster; (4) variants within genes that are not expressed in the testes were excluded; and (5)

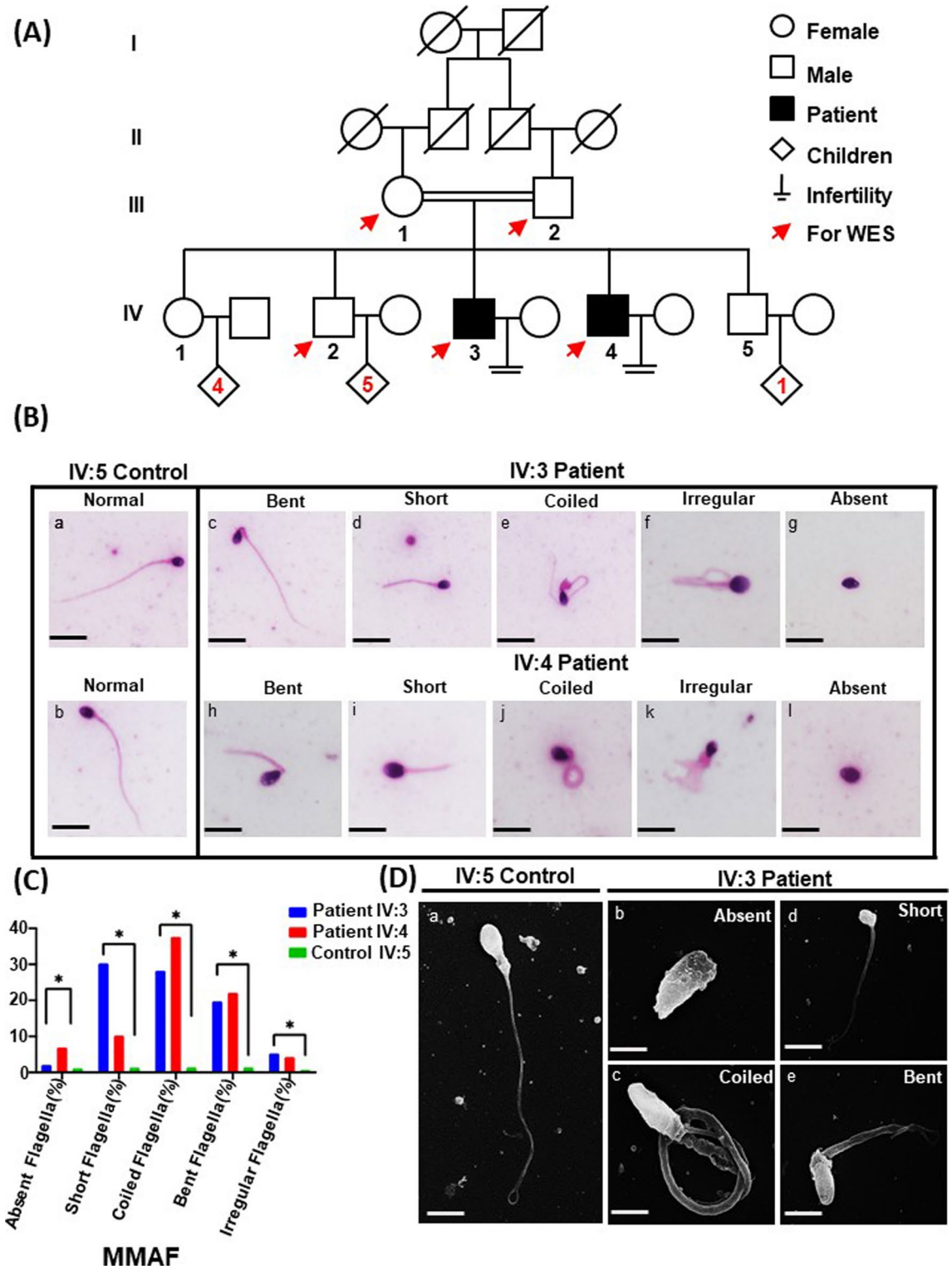

Fig. 1 Novel *NPHP4* missense variant causes infertility with MMAF in Pakistani consanguineous family. **A** Consanguineous family with two asthenozoospermia patients presenting MMAF phenotype. Filled symbols, infertile individuals; clear symbols, fertile individuals; double horizontal lines, consanguineous marriage; cross line, deceased; tetragon, multiple kids. **B** (a, b) Pap staining of spermatozoa from control IV:5 showing normal sperm morphology. Spermatozoa from patient IV:3 presenting MMAF phenotype, showing (c) bent, (d) short, (e) coiled, (f) irregular, and (g) absent. Spermatozoa from patient IV:4 presenting MMAF phenotype showing (h) bent, (i) short, (j) coiled, (k) irregular, and (l) absent. Scale bars 10 µm. **C** Statistical analysis of anomalies of sperm flagella from patient IV:3, IV:4 and control IV:5. **D** Scanning electron microscopy analysis (a) sperm from control IV:5, showing normal morphology. Sperm pictures from patient IV:3 indicated MMAF phenotype, showing (b) absent, (c) coiled, (d) short, and (e) bent flagella

variants within genes that may be important in spermatogenesis based on FertilityOnline or literature were included. Following a detailed WES analysis strategy, a novel variant in *NPHP4* was identified as the only potentially pathogenic variant in this family (c.1490C > G, p.P497R) (Figure S1). Subsequently, Sanger sequencing of further confirmed the identified mutation, which recessively co-segregating with the infertility phenotype in this family (Fig. 2B).

Pathogenicity of the novel mutation and its effect on the structure and function of *NPHP4*

The homozygous mutation at position 497 in exon 12 of NPHP4 results in the replacement of the residue proline (P) with arginine (R) (Fig. 2A). To assess the pathogenicity of this missense mutation (NPHP4P.497P > R), eleven different bioinformatics tools were used, including PolyPhen-1, PolyPhen-2, PROVEAN, SIFT, Align GV-GD, FATHMM, PhD-SNP, MAPP, Mutation Assessor, SNAP-2, and Mutation Taster. Nine of these tools predicted the mutation to be pathogenic, while one predicted a medium effect on NPHP4, as shown in Table S2. The multiple sequence alignment results showed that the altered amino acid (asparagine) is conserved among different species, indicating the functional importance of the $NPHP4^{P497R}$ mutation site (Fig. 2C). As approximately 70 to 80% of disease-causing variants in amino acid sequences are found in the secondary protein structure, it is crucial to understand any changes in the tertiary structure of the protein caused by the NPHP4P497R mutation. Therefore, the effect of this mutation on the protein structure was analyzed using HOPE and FoldX. The predicted structure of the mutant protein differed from that of the wild-type protein, suggesting that the identified mutation causes abnormalities in the structure and conservation of the NPHP4 gene (Fig. 3). Additionally, the impact of the proline-to-arginine mutation at position 497 was analyzed (Fig. 3C). Each amino acid has unique properties such as size, charge, and hydrophobicity. The original wild-type residue and the newly introduced mutant residue often differ in these properties. The mutant protein's structure was predicted to be altered compared to that of the wild-type protein, indicating that the identified mutation caused abnormalities in the NPHP4 protein's structure and conservation. The wild-type residue had a neutral charge, while the mutant residue had a positive charge. The hydrophobicity of the wild-type and mutant residues differed, with the wild-type residue being more hydrophobic than the mutant residue. Hydrophobic interactions either in the protein core or on the surface could be lost due to this change. Prolines are known to have a rigid structure that sometimes forces the backbone into a specific conformation, which could be required at this position. The $NPHP4^{P497R}$ mutation may change a proline with such a function into another residue, thereby disturbing the local structure. The mutant residue is larger, which may lead to bumps, and prolines are known to be rigid and therefore induce a special backbone conformation, which may be required at this position. The mutation can disturb this special conformation and cause repulsion of ligands or other residues with the same charge. Furthermore, we used the Mutant Pro and I-Mutant tools to analyze the effect of the mutation on the structural ability of the NPHP4 protein and predicted a decrease in the protein's stability due to the p.P497R mutation (Table S3). Therefore, the p.P497R mutation was possibly pathogenic and responsible for infertility in the patients. The results of the analyses suggest an essential role of this amino acid in the structure and function of the NPHP4 protein. Figure 3B shows the predicted aggregating regions in the protein structure. The empirical protein design force field FoldX was used to calculate the difference in the free energy of the mutation (ddG, delta delta G). The mutation from Pro to Arg at position 497 resulted in a ddG of 0.89 kcal/mol, indicating that the mutation has a detrimental effect on the stability of the protein, as illustrated in Fig. 3. In addition, we identified potential aggregating regions in the protein structure using the TANGO algorithm (Fig. 3B). Aggregating regions are regions of the protein that have a high propensity to aggregate, which can lead to the formation of insoluble protein aggregates and can cause protein misfolding and disease.

MMAF phenotype with loss of central pair confirmed by electron microscopy of patient spermatozoa

The notion that sperm mobility is impaired or reduced is typically accompanied by an abnormal morphology of the sperm. Light microscopy examination of patients' spermatozoa demonstrated that most of the spermatozoa (around 90%) had defective sperm flagella, such as missing, absent, or coiling with an asthenozoospermia phenotype. A scanning electron microscope was used to examine the spermatozoa of P1: IV:3 and the control brother IV:5. SEM analysis showed flagellar defects (Fig. 1D) that are compatible with Pap staining analysis and are consistent with astheno-ozoospermia. Additionally, we examined the ultrastructure of spermatozoa from the patients by examining TEM micrographs. Axonemes with 9 + 0 arrangements of microtubules were observed in patients (P1:IV:3) as compared with fertile controls, where the central pair was absent in mid-piece, principal, and endpiece sections (Fig. 4A). As a result of expanding our observation for a detailed analysis, we found that 100% of mid-piece sections, 89% of principal piece sections, and 92% of endpiece sections were abnormal (Fig. 4C). In summary, our study revealed that *NPHP4* (c.1490C > G, p.P497R) is associated with central pair loss and MMAF in patients with asthenozoospermia.

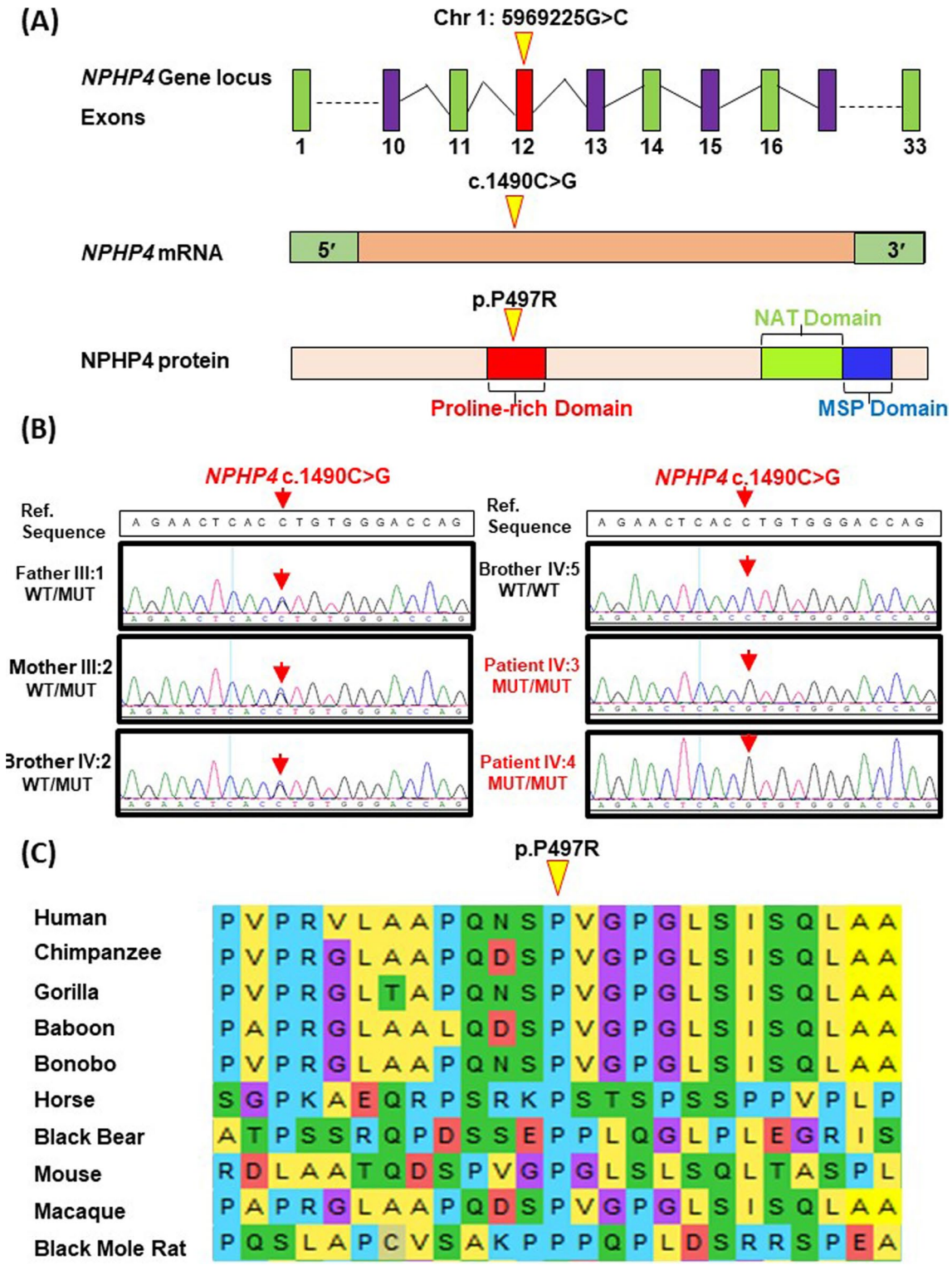

Fig. 2 Identification of *NPHP4* c.1490C > G homozygous pathogenic variant that co-segregated in both patients. **A** The identified NPHP4 mutation resulted in the c.1490C > G transversion in the coding sequence. This mutation (p.P497R) resulted in the replacement of proline "P" with arginine "R" at position 497. This (p.P497R) mutation is located in the proline rich domain of NPHP4 protein. **B** Sanger sequencing confirmed two infertile siblings (IV:3 and IV:4) contained a homozygous missense mutation (p.P497R) in NPHP4. Both parents (III:1 and III:2) and patients brother IV:5 carried heterozygous *NPHP4* mutation. Brother (IV:2) is wild type to the identified mutation. Red box showing the position of mutated nucleotides. **C** Multiple sequence alignment of the NPHP4 protein across different species, yellow color arrow head indicates the position of evolutionary conserved mutant residue p.P497R in the patients (IV:3 and IV:4). NAT, N-Acyltransferase; MSP, Major sperm protein

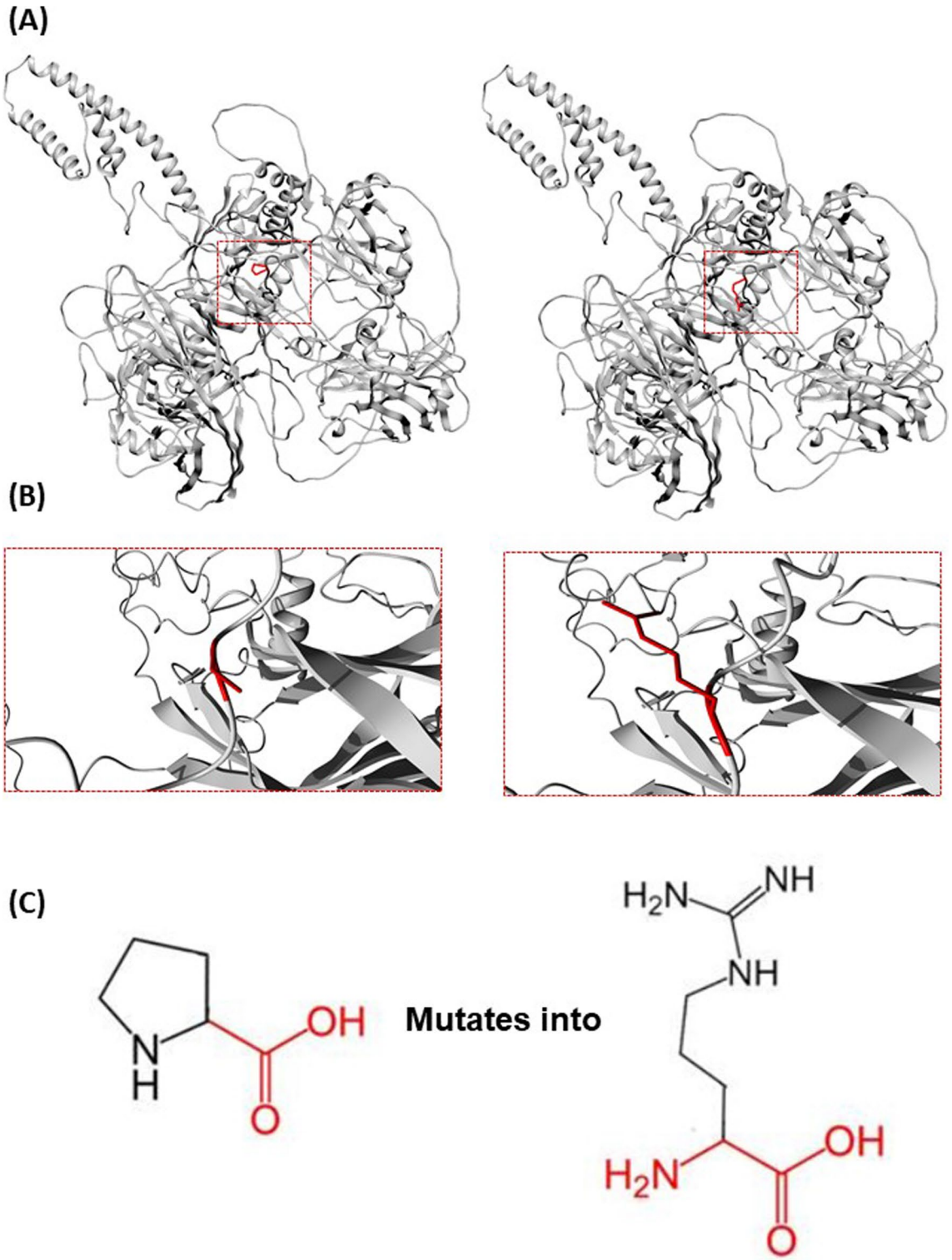

Fig. 3 Effect of mutation on NPHP4 stability Comparison of wild type NPHP4 protein structure with its mutant forms. **A** The structure of wild type NPHP4 protein and its mutant having mutation from proline to arginine at position 151. **B** Molecular visualization of the WT (left) and variant (right) amino acid. The residues colored in red represents the wild type [52] and variant residue (ARG). **C** The backbone, which is the same for each amino acid, is colored red. The side chain, which is unique for each amino acid, is colored black

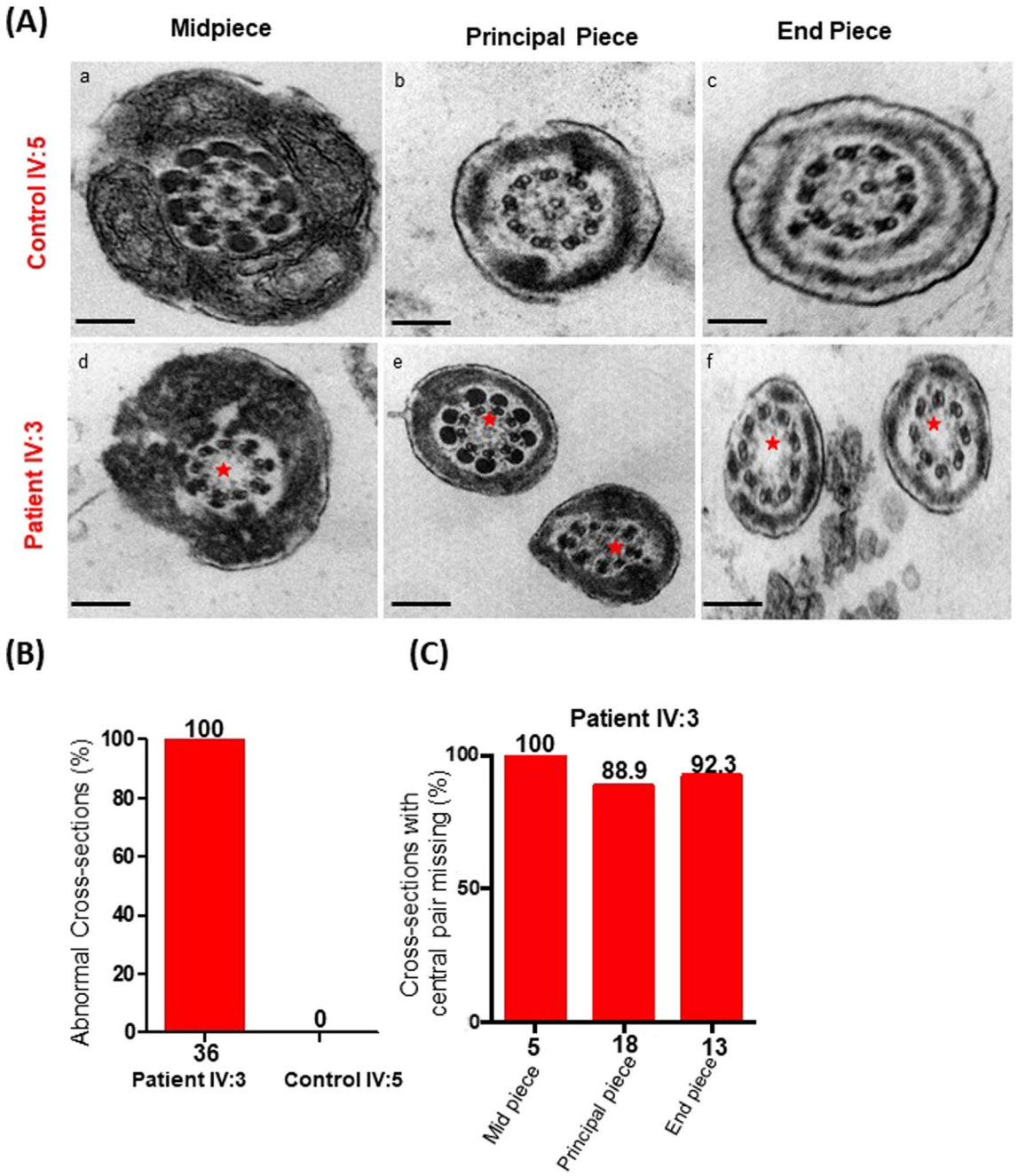

Fig. 4 Ultrastructure of control and patient spermatozoa carrying homozygous missense NPHP4 variant. **A** Transmission electron microscopy (TEM) analysis of sperm tail (a–c) cross-sections of a sperm flagellum from patient IV:3 shows a 9+0 axoneme lacking the CP (red asterisk) in (a) mid piece, (b) principal piece, and (c) end piece. (d–f) Cross-sections of the sperm flagellum from a control individual IV:5. (d) mid piece, (e) principal piece, and (f) end piece. The typical axoneme composed of nine doublets of microtubules (DMTs) organized circularly around a central-pair complex (CPC) of microtubules (9+2). This axoneme is composed of (7) outer dense fibers (ODFs) and fibrous sheath [18] containing (2) longitudinal columns (LCs) attached by circumferential ribs (CRs). Scale bars represent 200 nm [66]. **B** The number of abnormal cross-sections in patient IV:3 and control individual IV:5. **C** Number of cross-sections of mid piece, principal piece and end piece with Absence of central pair

Discussion

Several factors contribute directly to male infertility, including low sperm counts, decreased motility, and abnormal sperm morphology [12, 62]. Approximately 80% of male infertility cases are caused by impaired sperm motility, which is an important factor in normal fertilization. Also, sperm morphology plays an imperative role in sperm

movement, and a problem with sperm morphology contributes significantly to male infertility [63]. It was found that abnormalities in the morphology of spermatozoa resulted in wide ranges of phenotypes affecting the head, neck, mid piece, or tail of the spermatozoa. The phenotype of multiple morphological abnormalities of the sperm flagella (MMAF) corresponds to morphological abnormalities of the sperm flagellum, such as short, bent, coiled, irregular, or absent flagella [8, 64]. Almost all cases of MMAF are accompanied by visible ultrastructural defects and/or axonemal disorganization, resulting in aberrant morphology of sperm flagella that further effects motility or even cause sperm immobility [8, 65]. WES is widely used to identify the disease-causing mutations of human infertility due to the reduced costs of next-generation sequencing. In the present study, variants of infertile cases were filtered based on their segregation patterns within the families. Thus, the current study identified a genetic mutation c.1490C > G (p.P497R) in the *NPHP4* gene in a consanguineous Pakistani family suffering from male infertility due to MMAF, which was predicted to be deleterious by several *in silico* software [66].

Mollet et al. reported previously that *NPHP4* mutations in patients with NPHP represent the leading cause of kidney disease inherited in an autosomal recessive pattern and may also be associated with neurological abnormalities and/or vision disorders [17]. With the identification of the c.1490C > G transversion mutation of *NPHP4* in two siblings with MMAF phenotypes, this study expands the range of phenotypes associated with *NPHP4* variants.

Knockdown of *NPHP4* expression is associated with abnormal ciliogenesis and altered localization of ciliary proteins [67, 68]. Similarly, a truncating mutation induced by N-ethyl-N-nitrosourea (ENU) was shown to recapitulate the phenotype observed in 10% of nephronophthisis patients and surprise to everyone, it also displayed a unique reproductive phenotype not previously observed in humans. Mutant mice were infertile, and their sperm count and motility were significantly reduced. In particular, sperms from these mutant mice were not capable of fertilizing eggs in vitro, indicating that the cause of infertility extends beyond a reduced count and motility of sperms but also to abnormal sperm morphology [69]. Therefore, loss of function of *Nphp4* was strongly suggested to be responsible for reproductive barriers in mice, but the relationship between *NPHP4* variants and human male infertility must be explored. In our study patients, we have also observed a low sperm count and low sperm motility as well as an increased frequency of morphological abnormalities, predominantly multiple morphological abnormalities of sperm flagella (MMAF).

A study performed by Alazami et al. recently reported a homozygous truncated mutation in *NPHP4* (c.2044C > T, p.R682*) in a family with cerebello-oculo-renal syndrome and infertility in males. Analysis of sperm samples from patients revealed a highly viscous, low-volume sample containing few motile sperms and significant morphological abnormalities [18]. In contrast to these reports in mice and humans, our patients did not exhibit any other disease-related symptoms, such as nephronophthisis or retinal abnormalities, except mild proteinuria on routine urine examination. In addition to the decreased sperm count and motility, SEM and TEM analyses of sperm from *NPHP4* mutant patients revealed sperm flagella anomalies, particularly the absence of a central pair (9 + 0) of microtubules, which might be responsible for the MMAF phenotype. This study provides further support for the hypothesis that disorganization of the central pair of microtubules of the axoneme is the major factor giving rise to the MMAF phenotype, as this type of abnormality has previously been described as the most frequent ultrastructural abnormality observed in genetically uncharacterized MMAF patients [7, 70].

As a conclusion, we report the occurrence of the *NPHP4* c.1490C > G (p.P497R) mutation in a consanguineous Pakistani family with an asthenozoospermia phenotype, expanding the phenotypic spectrum of this mutation. This study contributes to our understanding of sperm flagellar abnormalities, including their etiology and pathophysiology associated with MMAF, and provides useful information for genetic counseling and the diagnosis of male infertility.

Supplementary information The online version contains supplementary material available at https://doi.org/10.1007/s10815-023-02966-x.

Author contribution QS: resources. AA, HZ, DS, BZ, and AM performed the experiments. AA, SH, KM, and KMBS recruited the patients and collected samples. AA, KR, ZM, and JX wrote the original draft. AU and AM performed *in silico* analysis. HZ and ZY performed the WES sequencing, Sanger sequencing, and WES analyses. QS: project administration and funding acquisition. All authors contributed to the article and approved the submitted version.

Funding This work was supported by the China's National Key Research and Development Program of China (2018YFC1003900, 2019YFA0802600), the China's National Foundation for Natural Sciences (82071709 and 31871514), and the Fundamental Research Funds for Central Universities (YD2070002006 and YD2070002012).

Declarations

Ethics approval The present study was approved by the Institutional Ethical Committee of the University of Science and Technology of China (USTC: Hefei, China) with the approval number UST-CEC202000003.

Competing interests The authors declare no competing interests.

References

1. Gershoni M, et al. A new MEIOB mutation is a recurrent cause for azoospermia and testicular meiotic arrest. Hum Reprod. 2019;34(4):666–71.

2. Farhi J, Ben-Haroush A. Distribution of causes of infertility in patients attending primary fertility clinics in Israel. Sat. 2011;4:19.
3. Rimoin DL, Connor JM, Pyeritz RE, Korf BR. Emery and Rimoin's principles and practice of medical genetics. Churchill Livingstone Elsevier; 2007.
4. Schultz N, Hamra FK, Garbers DL. A multitude of genes expressed solely in meiotic or postmeiotic spermatogenic cells offers a myriad of contraceptive targets. Proc Natl Acad Sci. 2003;100(21):12201–6.
5. Djureinovic D, et al. The human testis-specific proteome defined by transcriptomics and antibody-based profiling. Mol Hum Reprod. 2014;20(6):476–88.
6. Chemes HE. Phenotypes of sperm pathology: genetic and acquired forms in infertile men. J Androl. 2000;21(6):799–808.
7. Chemes HE, Rawe VY. Sperm pathology: a step beyond descriptive morphology. Origin, characterization and fertility potential of abnormal sperm phenotypes in infertile men. Hum Reprod Updat. 2003;9(5):405–28.
8. Khelifa MB, et al. Mutations in DNAH1, which encodes an inner arm heavy chain dynein, lead to male infertility from multiple morphological abnormalities of the sperm flagella. Am J Hum Genet. 2014;94(1):95–104.
9. Martinez G, et al. Whole-exome sequencing identifies mutations in FSIP2 as a recurrent cause of multiple morphological abnormalities of the sperm flagella. Hum Reprod. 2018;33(10):1973–84.
10. Lorès P, et al. Homozygous missense mutation L673P in adenylate kinase 7 (AK7) leads to primary male infertility and multiple morphological anomalies of the flagella but not to primary ciliary dyskinesia. Hum Mol Genet. 2018;27(7):1196–211.
11. Coutton C, et al. Bi-allelic mutations in ARMC2 lead to severe astheno-teratozoospermia due to sperm flagellum malformations in humans and mice. Am J Hum Genet. 2019;104(2):331–40.
12. Shen Y, et al. Loss-of-function mutations in QRICH2 cause male infertility with multiple morphological abnormalities of the sperm flagella. Nat Commun. 2019;10(1):433.
13. Ma H, et al. Novel frameshift mutation in STK33 is associated with asthenozoospermia and multiple morphological abnormalities of the flagella. Hum Mol Genet. 2021;30(21):1977–84.
14. Zhou Z, et al. A novel splicing variant in DNAH8 causes asthenozoospermia. J Assist Reprod Genet. 2021;38(6):1545–50.
15. Coutton C, et al. Teratozoospermia: spotlight on the main genetic actors in the human. Hum Reprod Update. 2015;21(4):455–85.
16. Liu C, et al. Bi-allelic DNAH8 variants lead to multiple morphological abnormalities of the sperm flagella and primary male infertility. Am J Hum Genet. 2020;107(2):330–41.
17. Mollet G, et al. The gene mutated in juvenile nephronophthisis type 4 encodes a novel protein that interacts with nephrocystin. Nat Genet. 2002;32(2):300.
18. Alazami A, et al. NPHP4 mutation is linked to cerebello-oculo-renal syndrome and male infertility. Clin Genet. 2014;85(4):371–5.
19. World Health Organization. WHO laboratory manual for the examination and processing of human semen, 5th ed. New York: World Health Organization; 2010;287.
20. Zhang B, Ma H, Khan T, Ma A, Li T, Zhang H, Gao J, Zhou J, Li Y, Yu C, Bao J, Ali A, Murtaza G, Yin H, Gao Q, Jiang X, Zhang F, Liu C, Khan I, Zubair M, Hussain HMJ, Khan R, Yousaf A, Yuan L, Lu Y, Xu X, Wang Y, Tao Q, Hao Q, Fang H, Cheng H, Zhang Y, Shi Q. A DNAH17 missense variant causes flagella destabilization and asthenozoospermia. J Exp Med. 2020;217(2):e20182365. https://doi.org/10.1084/jem.20182365.
21. Cindrić S, et al. SPEF2- and HYDIN-mutant cilia lack the central pair-associated protein SPEF2, aiding primary ciliary dyskinesia diagnostics. Am J Respir Cell Mol Biol. 2020;62(3):382–96.
22. Auton A, et al. A global reference for human genetic variation. Nature. 2015;526(7571):68–74.
23. Sukhai MA, et al. Somatic tumor variant filtration strategies to optimize tumor-only molecular profiling using targeted next-generation sequencing panels. J Mol Diagn. 2019;21(2):261–73.
24. Karczewski KJ, et al. The ExAC browser: displaying reference data information from over 60 000 exomes. Nucleic Acids Res. 2017;45(D1):840–5.
25. Tukiainen T, et al. Landscape of X chromosome inactivation across human tissues. Nature. 2017;550(7675):244–8.
26. Auger J, Jouannet P, Eustache F. Another look at human sperm morphology. Hum Reprod. 2016;31(1):10–23.
27. Sim NL, et al. SIFT web server: predicting effects of amino acid substitutions on proteins. Nucleic Acids Res. 2012;40(Web Server issue):W452–7.
28. Adzhubei IA, et al. A method and server for predicting damaging missense mutations. Nat Methods. 2010;7(4):248–9.
29. Schwarz JM, et al. MutationTaster2: mutation prediction for the deep-sequencing age. Nat Methods. 2014;11(4):361–2.
30. Reva B, Antipin Y, Sander C. Predicting the functional impact of protein mutations: application to cancer genomics. Nucleic Acids Res. 2011;39(17):e118.
31. Shihab HA, et al. Predicting the functional, molecular, and phenotypic consequences of amino acid substitutions using hidden Markov models. Hum Mutat. 2013;34(1):57–65.
32. Dong C, et al. Comparison and integration of deleteriousness prediction methods for nonsynonymous SNVs in whole exome sequencing studies. Hum Mol Genet. 2015;24(8):2125–37.
33. Davydov EV, et al. Identifying a high fraction of the human genome to be under selective constraint using GERP++. PLoS Comput Biol. 2010;6(12):e1001025.
34. Lindblad-Toh K, et al. A high-resolution map of human evolutionary constraint using 29 mammals. Nature. 2011;478(7370):476–82.
35. Gao J, Zhang H, Jiang X, Ali A, Zhao D, Bao J, Jiang L, Iqbal F, Shi Q, Zhang Y. FertilityOnline: Straightforward Pipeline for Functional Gene Annotation and Disease Mutation Discovery. Genomics Proteomics Bioinformatics. 2021;20(3):455–65. https://doi.org/10.1016/j.gpb.2021.08.010.
36. Bendl J, et al. PredictSNP: robust and accurate consensus classifier for prediction of disease-related mutations. PLoS Comput Biol. 2014;10(1):e1003440.
37. Ramensky V, Bork P, Sunyaev S. Human non-synonymous SNPs: server and survey. Nucleic Acids Res. 2002;30(17):3894–900.
38. Stone EA, Sidow A. Physicochemical constraint violation by missense substitutions mediates impairment of protein function and disease severity. Genome Res. 2005;15(7):978–86.
39. Ng PC, Henikoff S. SIFT: Predicting amino acid changes that affect protein function. Nucleic Acids Res. 2003;31(13):3812–4.
40. Bromberg Y, Rost B. SNAP: predict effect of non-synonymous polymorphisms on function. Nucleic Acids Res. 2007;35(11):3823–35.
41. Bao L, Zhou M, Cui Y. nsSNPAnalyzer: identifying disease-associated nonsynonymous single nucleotide polymorphisms. Nucleic Acids Res. 2005;33(Web Server issue):W480–2.
42. Sim NL, et al. SIFT web server: predicting effects of amino acid substitutions on proteins. Nucleic Acids Res. 2012;40(Web Server issue):W452–7.
43. Choi Y, Chan AP. PROVEAN web server: a tool to predict the functional effect of amino acid substitutions and indels. Bioinformatics. 2015;31(16):2745–7.

44. Tavtigian SV, et al. Comprehensive statistical study of 452 BRCA1 missense substitutions with classification of eight recurrent substitutions as neutral. J Med Genet. 2006;43(4):295–305.
45. Capriotti E, et al. Predicting protein stability changes from sequences using support vector machines. Bioinformatics. 2005;21(Suppl 2):ii54-8.
46 Capriotti E, Fariselli P, Casadio R. I-Mutant2.0: predicting stability changes upon mutation from the protein sequence or structure. Nucleic Acids Res. 2005;33(Web Server issue):W306-10.
47. Altschul SF, et al. Gapped BLAST and PSI-BLAST: a new generation of protein database search programs. Nucleic Acids Res. 1997;25(17):3389–402.
48. Li W, Jaroszewski L, Godzik A. Clustering of highly homologous sequences to reduce the size of large protein databases. Bioinformatics. 2001;17(3):282–3.
49 Fang H, Gough J. DcGO: database of domain-centric ontologies on functions, phenotypes, diseases and more. Nucleic Acids Res. 2013;41(Database issue):D536-44.
50. Gough J, et al. Assignment of homology to genome sequences using a library of hidden Markov models that represent all proteins of known structure. J Mol Biol. 2001;313(4):903–19.
51. Reva B, Antipin Y, Sander C. Determinants of protein function revealed by combinatorial entropy optimization. Genome Biol. 2007;8(11):R232.
52. Flicek P, et al. Ensembl 2012. Nucleic Acids Res. 2012;40(Database issue):D84–90.
53 Hecht M, Bromberg Y, Rost B. Better prediction of functional effects for sequence variants. BMC Genomics. 2015;16(Suppl 8):S1.
54. Berman HM, et al. The protein data bank. Nucleic Acids Res. 2000;28(1):235–42.
55 Bava KA, et al. ProTherm, version 4.0: thermodynamic database for proteins and mutants. Nucleic Acids Res. 2004;32(Database issue):D120-1.
56. Kabsch W, Sander C. Dictionary of protein secondary structure: pattern recognition of hydrogen-bonded and geometrical features. Biopolymers. 1983;22(12):2577–637.
57. Chothia C. The nature of the accessible and buried surfaces in proteins. J Mol Biol. 1976;105(1):1–12.
58. Cheng J, Randall A, Baldi P. Prediction of protein stability changes for single-site mutations using support vector machines. Proteins. 2006;62(4):1125–32.
59. Venselaar H, et al. Protein structure analysis of mutations causing inheritable diseases. An e-Science approach with life scientist friendly interfaces. BMC Bioinforma. 2010;11:548.
60. Saitou N, Nei M. The neighbor-joining method: a new method for reconstructing phylogenetic trees. Mol Biol Evol. 1987;4(4):406–25.
61. Kumar S, et al. MEGA X: molecular evolutionary genetics analysis across computing platforms. Mol Biol Evol. 2018;35(6):1547–9.
62. Haxton M, Fleming R, Coutts J. Population study of causes, treatment, and outcome of infertility. Br Med J (Clin Res Ed). 1986;292(6515):272.
63. Curi S, et al. Asthenozoospermia: analysis of a large population. Arch Androl. 2003;49(5):343–9.
64. Yang S-M, et al. Morphological characteristics and initial genetic study of multiple morphological anomalies of the flagella in China. Asian J Androl. 2015;17(3):513.
65. Tang S, et al. Biallelic mutations in CFAP43 and CFAP44 cause male infertility with multiple morphological abnormalities of the sperm flagella. Am J Hum Genet. 2017;100(6):854–64.
66. Krausz C, Riera-Escamilla A. Genetics of male infertility. Nat Rev Urol. 2018;15(6):369–84.
67. Mollet G, et al. Characterization of the nephrocystin/nephrocystin-4 complex and subcellular localization of nephrocystin-4 to primary cilia and centrosomes. Hum Mol Genet. 2005;14(5):645–56.
68. Delous M, et al. Nephrocystin-1 and nephrocystin-4 are required for epithelial morphogenesis and associate with PALS1/PATJ and Par6. Hum Mol Genet. 2009;18(24):4711–23.
69. Won J, et al. NPHP4 is necessary for normal photoreceptor ribbon synapse maintenance and outer segment formation, and for sperm development. Hum Mol Genet. 2010;20(3):482–96.
70. Coutton C, Arnoult C, Ray PF. Commentary on "morphological characteristics and initial genetic study of multiple morphological anomalies of the flagella in China." Asian J Androl. 2016;18(5):812.